

# Gardner optimal capacity of the diluted Blume-Emery-Griffiths neural network

D. Bollé\* and I. Pérez Castillo†

*Instituut voor Theoretische Fysica, Katholieke Universiteit Leuven, B-3001 Leuven, Belgium*

The optimal capacity of a diluted Blume-Emery-Griffiths neural network is studied as a function of the pattern activity and the embedding stability using the Gardner entropy approach. Annealed dilution is considered, cutting some of the couplings referring to the ternary patterns themselves and some of the couplings related to the active patterns, both simultaneously (synchronous dilution) or independently (asynchronous dilution). Through the de Almeida-Thouless criterion it is found that the replica-symmetric solution is locally unstable as soon as there is dilution. The distribution of the couplings shows the typical gap with a width depending on the amount of dilution, but this gap persists even in cases where a particular type of coupling plays no role in the learning process.

PACS numbers: 02.50.-r, 64.60.Cn, 75.10.Hk, 87.18.Sn

## I. INTRODUCTION

During recent years the Blume-Emery-Griffiths (BEG) model [1] has been studied quite intensively in the context of neural networks, one of the reasons being that it was argued in [2] that this model maximizes the mutual information content of three-state networks with Hebbian-type learning rules. To know in more detail how the retrieval quality of the BEG network compares with other three-state neuron models, the thermodynamics of this model was studied and temperature-capacity phase diagrams were obtained [3]. It was shown that the retrieval phase is systematically larger than that of other three-state models and that the critical capacity is about twice as large as that of the three-state neuron Ising model [4]. Also the region of thermodynamic stability is much larger and, furthermore, the phase diagram itself is much richer with the presence of a stable quadrupolar state, carrying also retrieval information, at high temperatures.

It was also shown that this enhancement of the retrieval properties is not restricted to the use of the Hebbian learning rule but that it is inherent to the model. Indeed, by studying the Gardner optimal capacity [5] in replica symmetric (RS) mean-field theory it was found recently [6] that for the corresponding BEG perceptron with, e.g., zero embedding stability parameter and uniform patterns this capacity is 2.24. Comparing with other three-state neuron perceptron models, we recall that for the  $Q = 3$  Ising perceptron the Gardner optimal capacity can maximally reach 1.5 [7, 8], whereas for the  $Q = 3$  clock and Potts model both reach an optimal capacity of 2.40 [9, 10]. At this point we have to remark that the  $Q = 3$  Ising perceptron and the BEG perceptron have the same topology structure in the neurons, whereas the  $Q = 3$  clock and Potts models have different topologies. For the Ising topology structure the BEG-perceptron has the best performance.

The interesting question remains whether and in how far these enhanced retrieval properties are robust against dilution. Studying this question is the aim of the present work. Besides the fact that the connectivity of biological networks is far from complete, diluted networks offer the possibility to study the robustness against malfunctioning of some of the connections. Furthermore, in asymmetric architectures they reduce the internal feedback correlations of fully connected networks making a complete analytic description of the dynamics much easier [2], [11, 12]. Finally, in the BEG perceptron there are two sets of couplings, those referring to the three-state patterns themselves and those related to the active, i.e., the non-zero patterns. By diluting both types of couplings simultaneously or diluting these couplings independently, we can study, in particular, the influence of the active patterns on the Gardner optimal capacity of the BEG perceptron. These results can be obtained in closed analytic form.

We remark that the type of dilution we study in this paper is such that the number of connections to a given site still increases with the size of the system. In the replica approach to capacity problems for these systems, only order parameters with two replica indices appear. Recently, the study of neural networks with finite connectivity, i.e., where the number of connections to a given site remains finite in the thermodynamic limit has been started [13, 14]. There, functional order parameters have to be introduced.

The paper is organized as follows. In Sect. II we recall the BEG model and briefly discuss some of its properties. In Sect. III we introduce the different kinds of dilution that one may study and report on the application of the Gardner approach to these cases. We present the results for the optimal capacity in the RS approximation as a function of the pattern activity, the stability parameter and the degree of dilution. In Sect. IV we discuss the results for the distribution of the couplings and in Sect. V we study the validity of the local stability criterion for the RS solution. The last section contains the conclusions.

\*Electronic address: Desire.Bolle@fys.kuleuven.ac.be

†Electronic address: Isaac.Perez@fys.kuleuven.ac.be

## II. THE BEG NEURAL NETWORK

Let us consider a neural network consisting of  $N$  neurons which can take values  $\sigma_i, i = 1, \dots, N$  from the discrete set  $\mathcal{S} \equiv \{-1, 0, +1\}$ . The  $p$  patterns to be stored in this network are supposed to be a collection of independent and identically distributed random variables (i.i.d.r.v.),  $\xi_i^\mu, \mu = 1, \dots, p$ , taken from the set  $\mathcal{S}$  with a probability distribution

$$p(\xi_i^\mu) = \frac{a}{2}\delta(\xi_i^\mu - 1) + \frac{a}{2}\delta(\xi_i^\mu + 1) + (1 - a)\delta(\xi_i^\mu) \quad (1)$$

with  $a$  the activity of the patterns so that

$$\lim_{N \rightarrow \infty} \frac{1}{N} \sum_i (\xi_i^\mu)^2 = a. \quad (2)$$

Given the network configuration at time  $t$ ,  $\sigma_N \equiv \{\sigma_j(t)\}, j = 1, \dots, N$ , the following dynamics is considered. The configuration  $\sigma_N(0)$  is chosen as input. The neurons are updated according to the stochastic parallel spin-flip dynamics defined by the transition probabilities

$$\begin{aligned} \Pr(\sigma_i(t+1) = s' \in \mathcal{S} | \sigma_N(t)) \\ = \frac{\exp[-\beta \epsilon_i(s' | \sigma_N(t))]}{\sum_{s \in \mathcal{S}} \exp[-\beta \epsilon_i(s | \sigma_N(t))]} \cdot (3) \end{aligned}$$

Here the energy potential  $\epsilon_i[s | \sigma_N(t)]$  is defined by

$$\epsilon_i[s | \sigma_N(t)] = -s h_i(\sigma_N(t)) - s^2 \theta_i(\sigma_N(t)), \quad (4)$$

where the local fields in neuron  $i$ ,  $h_{N,i}(t) \equiv h_i(\sigma_N(t))$  carry all the information

$$h_{N,i}(t) = \sum_{j \neq i} J_{ij} \sigma_j(t), \quad \theta_{N,i}(t) = \sum_{j \neq i} K_{ij} \sigma_j^2(t). \quad (5)$$

At zero temperature the updating rule of this dynamics (3)-(4) is equivalent to the gain function formulation

$$\begin{aligned} \sigma_i(t+1) &= \text{sign}(h_{N,i}(t)) \Theta(|h_{N,i}(t)| + \theta_{N,i}(t)) \\ &\equiv g(h_{N,i}(t), \theta_{N,i}(t)) \end{aligned} \quad (6)$$

with  $\Theta(x)$  and  $\text{sign}(x)$  the Heaviside and the sign function, respectively.

Concerning the loading capacity of this model, the following results have appeared in the literature. For Hebbian-type synaptic couplings  $J_{ij}$  and  $K_{ij}$

$$J_{ij} = \frac{1}{a^2 N} \sum_{\mu=1}^p \xi_i^\mu \xi_j^\mu \quad (7)$$

$$K_{ij} = \frac{1}{a^2 (1-a)^2 N} \sum_{\mu=1}^p [(\xi_i^\mu)^2 - a][(\xi_j^\mu)^2 - a] \quad (8)$$

the long-time behavior is governed by the Hamiltonian

$$H = -\frac{1}{2} \sum_{i \neq j} J_{ij} \sigma_i \sigma_j - \frac{1}{2} \sum_{i \neq j} K_{ij} \sigma_i^2 \sigma_j^2, \quad (9)$$

and the retrieval properties are enhanced [3] in comparison to other three-state neuron models. In particular, the retrieval phase is systematically larger than that of other three-state models and the critical capacity is about twice as large as that of the three-state neuron Ising model. Moreover, depending on the value of the pattern activity a stable quadrupolar state carrying also non-zero retrieval information arises at high temperatures. However, an underlying reason why there is such an enlargement of the basin of attraction and hence of the retrieval properties of the network seems still to be absent.

This enhancement of retrieval has also been found [6] for the BEG-perceptron

$$\xi_0^\mu = \text{sgn}(h^\mu) \Theta(|h^\mu| + \theta^\mu), \quad \forall \mu = 1, \dots, p \quad (10)$$

with  $\xi_0^\mu$  denoting the output, and where  $h^\mu$  and  $\theta^\mu$  are the local fields at the output created by the pattern  $\mu$

$$h^\mu = \frac{1}{\sqrt{N}} \sum_{i=1}^N J_i \xi_i^\mu, \quad \theta^\mu = \frac{1}{\sqrt{N}} \sum_{i=1}^N K_i (\xi_i^\mu)^2 \quad (11)$$

with  $J_i, K_i$  a set of couplings connecting the input with the output. In a RS analysis the Gardner optimal capacity for this perceptron is calculated analytically and seen to be bigger than that of the  $Q = 3$ -Ising perceptron [7, 8].

## III. THE DILUTED BEG PERCEPTRON

We want to find out in how far these enhanced retrieval properties are robust against dilution. One of the questions we want to answer then is the following. Let  $\xi_i^\mu, \mu = 1, \dots, p, i = 0, \dots, N$  be an extensive set of  $p = \alpha N$  patterns supposed to be fixed points of the dynamical rule (10) where the local fields  $h^\mu$  and  $\theta^\mu$  are now given by

$$h^\mu = \frac{1}{\sqrt{c_J N}} \sum_{i=1}^N c_i^J J_i \xi_i^\mu, \quad \theta^\mu = \frac{1}{\sqrt{c_K N}} \sum_{i=1}^N c_i^K K_i (\xi_i^\mu)^2. \quad (12)$$

The parameters  $c_i^J \in \{0, 1\}$  and  $c_i^K \in \{0, 1\}$  control the presence of the connections  $J_i$  and  $K_i$ . We want to find a set of couplings,  $J_i^*, K_i^*$ , or equivalently, a BEG-perceptron with an average dilution  $c_J$  and  $c_K$

$$c_J = \frac{1}{N} \sum_{i=1}^N c_i^J, \quad c_K = \frac{1}{N} \sum_{i=1}^N c_i^K \quad (13)$$

that still fulfil the conditions (10). It is clear that for small values of the capacity  $\alpha$  more than one BEG-perceptron storing these patterns can be found. The bigger the value of  $\alpha$  the more difficult this task becomes and a saturation limit, called Gardner optimal capacity, is reached.

In the following we study dilution during learning, i.e., annealed dilution, which can be realized in two different

ways. The first one, called synchronous dilution, assumes that  $c_i^J = c_i^K \equiv c_i$  and, hence  $c_J = c_K$ ; the second one, named asynchronous dilution, allows the  $c_i$ 's to be different. Looking back at (12) we see that the  $c_i^J$  control the connections of the three-state patterns, while the  $c_i^K$  control the connections related to the active, i.e., the non-zero patterns. In fact, for Hebbian learning in (7)-(9) the  $K$ -couplings control the fluctuations around these active patterns. Therefore, by allowing synchronous or asynchronous dilution we can study the influence of the active patterns on the optimal capacity of the BEG perceptron.

### A. Synchronous dilution

To study the optimal capacity, we follow the entropy approach introduced by Gardner [5]. Since the dynamical variables are continuous, entropy has only meaning relatively and we write the volume  $V$  of all possible BEG-perceptrons satisfying (10), without normalizing, as

$$V = \prod_{i=1}^N \text{tr}_{c_i, J_i, K_i} \prod_{\mu=1}^p \chi_{\xi_0^\mu}(h^\mu, \theta^\mu; \kappa) \quad (14)$$

with  $\chi_{\xi_0^\mu}(h^\mu, \theta^\mu; \kappa)$  the characteristic function given by

$$\begin{aligned} \chi_{\xi_0^\mu}(h^\mu, \theta^\mu; \kappa) = & (\xi_0^\mu)^2 \Theta(\xi_0^\mu h^\mu - \kappa) \Theta(|h^\mu| + \theta^\mu - \kappa) \\ & + [1 - (\xi_0^\mu)^2] \Theta(-|h^\mu| - \theta^\mu - \kappa) \end{aligned} \quad (15)$$

where  $\kappa$  is the embedding stability parameter. Since we consider continuous couplings we need to introduce a modified spherical constraint

$$\sum_{i=1}^N c_i J_i^2 = cN, \quad \sum_{i=1}^N c_i K_i^2 = cN. \quad (16)$$

From this spherical constraint we see that the couplings are not well normalized at those sites where  $c_i$  is zero. One can solve this difficulty either by introducing an extra spherical constraint for the remaining couplings [15], either by restricting the trace over the couplings [16]. We take the second solution and define the restricted trace as

$$\text{tr}_{c_i, J_i, K_i}(\cdots) \equiv \sum_{c_i=0,1} \delta_{c_i,0}(\cdots) + \sum_{c_i=0,1} \delta_{c_i,1} \int dJ_i dK_i (\cdots). \quad (17)$$

Since we want to study typical features of the system the important quantity to average over is the entropy. Employing replica techniques [17] we express the entropy per neuron as

$$v = \lim_{N \rightarrow \infty} \lim_{n \rightarrow 0} \frac{1}{nN} \ln \langle V^n \rangle \quad (18)$$

where  $\langle \cdot \rangle$  denotes the average over the pattern distribution (1) and where  $V^n$  is the  $n$ -th times replicated volume of solutions

$$V^n = \left[ \prod_{j=1}^N \prod_{\alpha=1}^n \text{tr}_{c_i^\alpha, J_i^\alpha, K_i^\alpha} \right] \left[ \prod_{\alpha=1}^n \delta \left( \sum_{i=1}^N c_i^\alpha (J_i^\alpha)^2 - cN \right) \delta \left( \sum_{i=1}^N c_i^\alpha (K_i^\alpha)^2 - cN \right) \delta \left( \sum_{i=1}^N c_i^\alpha - cN \right) \right] \prod_{\mu=1}^p \prod_{\alpha=1}^n \chi_{\xi_0^\mu}(h_\alpha^\mu, \theta_\alpha^\mu; \kappa). \quad (19)$$

The further analysis then proceeds in a standard way although the technical details are much more involved. A short account is given in Appendix A.

The results are described essentially in terms of three order parameters, the first one,  $q_{\alpha\beta}$ , defined as the overlaps between two distinct replicas for the couplings  $J_i$ , the second one,  $r_{\alpha\beta}$ , a similar quantity for the couplings  $K_i$  and the third one,  $L^\alpha$ , arising from the fact that the dynamics and, hence, also the characteristic function contains a second field  $\theta$ , quadratic in the patterns (see (48)). In the RS approximation we are discussing here they are given by  $q_{\alpha\beta} = q, r_{\alpha\beta} = r, L^\alpha = L$ .

The RS Gardner optimal capacity is obtained when the overlap order parameters  $q$  and  $r$  go to 1. It is clear that these limits have to be taken simultaneously but, in general, their rate of convergence could be different. Therefore, we introduce  $(1-r) = \gamma(1-q)$  where  $\gamma$  is a new parameter which one also needs to extremize. We expect this parameter  $\gamma$  to depend on the pattern distribution

through the activity  $a$ . The result for the replica symmetric Gardner optimal capacity  $\alpha_{\text{syn}}^{RS}$  then reads

$$\alpha_{\text{syn}}^{RS}(a, \kappa, c) = \text{extr}_{u, L, \gamma} \frac{A_{\text{syn}}(u, \gamma; c)}{g(\gamma, L; a, \kappa)} \quad (20)$$

where the function  $A_{\text{syn}}(u, c; \gamma)$  is defined by

$$A_{\text{syn}}(u, \gamma; c) = u^2 c + A_{\text{syn}}^{(2)}(u, \gamma). \quad (21)$$

Stationarity with respect to  $u$  then leads to  $c = A_{\text{syn}}^{(1)}(u, \gamma)$ . Here the functions  $A_{\text{syn}}^{(m)}$ ,  $m = 1, 2$  are given by

$$A_{\text{syn}}^{(m)}(u, \gamma) = \frac{m\sqrt{\gamma}}{2\pi} \int_0^{2\pi} d\varphi \frac{\exp[-\frac{u^2}{2}(\cos^2 \varphi + \gamma \sin^2 \varphi)]}{(\cos^2 \varphi + \gamma \sin^2 \varphi)^m}. \quad (22)$$

The function  $g(\gamma, L; a, \kappa)$  in (20) can be expressed as

$$\begin{aligned}
g(\gamma, L; a, \kappa) = & a \sum_{i=1}^3 \int_{\mathcal{R}_i} \mathcal{D}(h_0 + \kappa/\sqrt{a}) \mathcal{D}(\sqrt{\gamma}\theta_0 - l_0) d_{min}^{\mathcal{R}_i}(h_0, \theta_0) \\
& + (1-a) \sum_{i=1}^3 \int_{\mathcal{R}'_i} \mathcal{D}(h_0) \mathcal{D}(\sqrt{\gamma}\theta_0 - l_\kappa) d_{min}^{\mathcal{R}'_i}(h_0, \theta_0)
\end{aligned} \tag{23}$$

with  $l_\kappa \equiv (aL + \kappa)/\sqrt{a(1-a)}$  and  $\mathcal{D}(ax+b) = (2\pi)^{-1/2} a \exp[(-1/2)(ax+b)^2] dx$ .

The integration regions are the following ones

$$\mathcal{R}_1 = \begin{cases} h_0 < 0 \\ \theta_0 > 0 \end{cases} \quad \mathcal{R}_2 = \begin{cases} h_0\gamma' < \theta_0 < 0 \\ h_0 < 0 \end{cases} \quad \mathcal{R}_3 = \begin{cases} \theta_0 < 0 \\ \theta_0/\gamma' < h_0 < -\theta_0\gamma' \end{cases} \tag{24}$$

$$\mathcal{R}'_1 = \begin{cases} h_0 > 0 \\ -h_0/\gamma' < \theta_0 < \gamma'h_0 \end{cases} \quad \mathcal{R}'_2 = \begin{cases} -\theta_0/\gamma' < h_0 < \theta_0/\gamma' \\ \theta_0 > 0 \end{cases} \quad \mathcal{R}'_3 = \begin{cases} h_0 < 0 \\ h_0/\gamma' < \theta_0 < -\gamma'h_0 \end{cases} \tag{25}$$

and the corresponding integrands are given by

$$d_{min}^{\mathcal{R}_1} = h_0^2 \quad d_{min}^{\mathcal{R}_2} = h_0^2 + \theta_0^2 \quad d_{min}^{\mathcal{R}_3} = \frac{1}{1+(\gamma')^2} (h_0 + \gamma'\theta_0)^2 \tag{26}$$

$$d_{min}^{\mathcal{R}'_1} = \frac{1}{1+(\gamma')^2} (h_0 + \gamma'\theta_0)^2 \quad d_{min}^{\mathcal{R}'_2} = h_0^2 + \theta_0^2 \quad d_{min}^{\mathcal{R}'_3} = \frac{1}{1+(\gamma')^2} (h_0 - \gamma'\theta_0)^2 \tag{27}$$

with  $\gamma' \equiv \sqrt{\gamma(1-a)}$ .

After inserting (23)-(27) in (20) and extremizing numerically we find the results presented in Fig. 1. We plot the optimal capacity  $\alpha(a, \kappa, c)$  itself (insets) and its values normalized by the optimal capacity for no dilution,  $\alpha(a, \kappa, c)/\alpha(a, \kappa, 1)$ , as a function of the dilution  $c$  for  $\kappa = 0$  and several values of the activity  $a$ .

We see that different regions of activities lead to different results. For small activities  $a \leq 0.5$  and hence, many inactive neurons, the optimal capacity strongly increases for decreasing dilution. This seems to be in agreement with what is known in the literature for very small activities or so-called sparse coding (see, e.g., [18], [19], [20]). When normalizing these results by  $\alpha(a, \kappa, 1)$  we find that all the lines collapse into the full line. For large activities  $a \geq 0.6$  and, hence, many active states  $\pm 1$ , the results for  $\alpha(a, \kappa, c)$  are only weakly dependent on the activity (see inset) but the results for the normalized optimal capacity do not collapse. Furthermore, we see that the network is more robust against synchronous dilution for non-sparse coding, i.e., for activities ranging in the interval  $[0.2, 1.0]$ : the dilution  $c$  can decrease from 1 to about 0.4 before one sees a substantial decrease in the optimal capacity. Comparing to the  $Q = 3$  Ising perceptron [16], the effect of dilution, especially for larger activities is about the same.

When  $c = 1$  ( $u = 0$ ), the functions  $A_{\text{syn}}^{(m)}(u, \gamma)$  can be explicitly integrated leading to

$$A_{\text{syn}}^{(1)}(0, \gamma) = 1, \quad A_{\text{syn}}^{(2)}(0, \gamma) = 1 + \frac{1}{\gamma} \tag{28}$$

and one recovers the optimal capacity found in the fully connected case [6]. When the pattern activity  $a$  goes to 1 the system is forced into two possible states, as in the Gardner model with dilution [15]. Since the overlap parameter  $r$  becomes irrelevant in such a limit  $\gamma$  must go to infinity. The numerical solution does confirm this. Furthermore, in this limit the functions  $A_{\text{syn}}^{(m)}(u, \gamma)$  become

$$\begin{aligned}
A_{\text{syn}}^{(1)}(u, \infty) &= \text{erfc}\left(\frac{u}{\sqrt{2}}\right) \\
A_{\text{syn}}^{(2)}(u, \infty) &= \frac{2u}{\sqrt{2\pi}} \exp\left(-\frac{u^2}{2}\right) + (1-u^2) \text{erfc}\left(\frac{u}{\sqrt{2}}\right)
\end{aligned}$$

and hence

$$A_{\text{syn}}(u, \infty; c) = c + \frac{2u}{\sqrt{2\pi}} \exp\left(-\frac{u^2}{2}\right). \tag{29}$$

These are precisely the Gardner results with dilution [15] after rescaling  $u/\sqrt{2} \rightarrow u$ . We remark that in this case, and also for the  $Q$ -Ising type models [16], it is possible to rescale the optimal capacity as follows

$$\frac{\alpha_{\text{syn}}^{RS}(\kappa, c)}{\alpha_{\text{syn}}^{RS}(\kappa, c=1)} = c + \frac{2u}{\sqrt{2\pi}} \exp\left(-\frac{u^2}{2}\right) \tag{30}$$

with  $c = \text{erfc}(u/\sqrt{2})$ . For the general BEG-perceptron treated here such a scaling is not possible because the factor  $\gamma$  appears both in the numerator and denominator of Eq.(20). It is possible, however, to derive the bound

$$c - c \log c \leq \frac{\alpha_{RS}(\kappa, a, c)}{\alpha_{RS}(\kappa, a, c=1)} \leq c + \frac{2u}{\sqrt{2\pi}} \exp\left(-\frac{u^2}{2}\right) \tag{31}$$

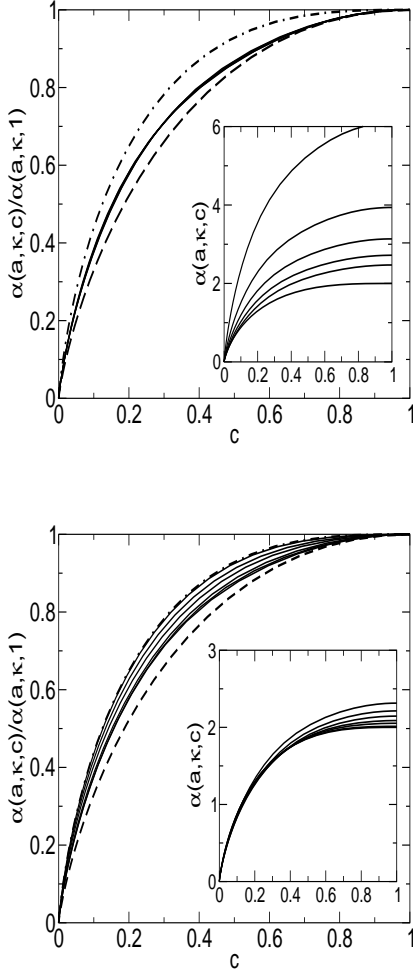


FIG. 1: Optimal capacity for synchronous dilution in the BEG-perceptron as a function of  $c$  for  $\kappa = 0$  and several values of  $a$ . Top figure: the normalized optimal capacity (solid line), its upper bound (dashed-dotted line) and its lower bound (broken line); the inset displays  $\alpha(a, \kappa, c)$  for  $a = 0.1, 0.2, 0.3, 0.4, 0.5$  from top to bottom. Bottom figure : similar to the top figure for  $a = 0.6, 0.7, 0.8, 0.9, 0.95, 0.99$ .

for  $0 \leq a \leq 1$  with  $c$  and  $u$  related through  $c = \text{erfc}(u/\sqrt{2})$ . These bounds are shown in Fig. 1 as the broken line (lower bound) and the dashed-dotted line (upper bound). Although the dependence on the dilution and other parameters is not that simple, we do find that the dependence on the embedding stability parameter  $\kappa$  is rather weak.

### B. Asynchronous dilution

In this case  $c_J$  is different from  $c_K$  allowing us to study the relative influence of the two sets of couplings. An analogous calculation as the one in subsection A can be done leading to the following result for the optimal capacity

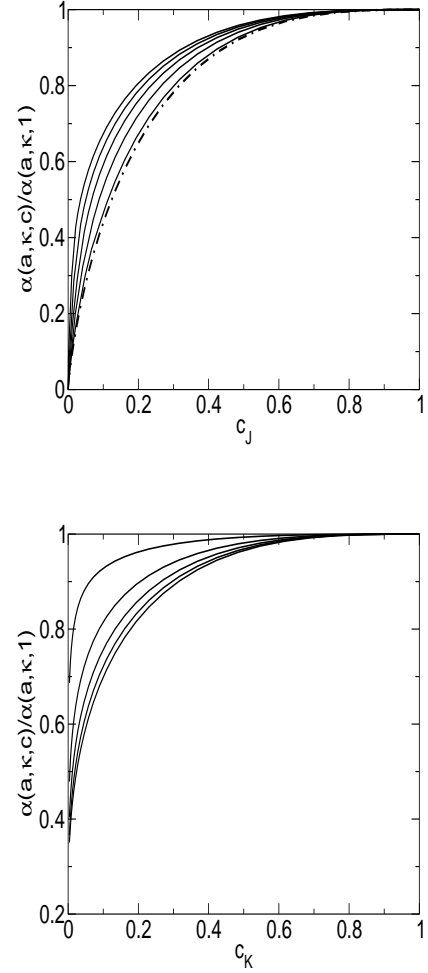


FIG. 2: Optimal capacity for asynchronous dilution in the BEG-perceptron. Top figure: the normalized optimal capacity as a function of  $c_J$  for  $c_K = 1$ ,  $\kappa = 0.0$  and activity  $a = 0.1, 0.3, 0.5, 0.7, 0.9$  from top to bottom. The dashed-dotted line is for  $a = 1$ . Bottom figure: the normalized capacity as a function of  $c_K$  for  $c_J = 1$ ,  $\kappa = 0.0$  and pattern activity  $a = 0.1, 0.3, 0.5, 0.7, 0.9$  from bottom to top.

$$\alpha_{\text{asyn}}^{RS}(a, \kappa, c_J, c_K) = \underset{u_J, u_K, L, \gamma}{\text{extr}} \frac{A_{\text{asyn}}(u_J; c_J) + \frac{1}{\gamma} A_{\text{asyn}}(u_K; c_K)}{g(\gamma, L; a, \kappa)} \quad (32)$$

with

$$A_{\text{asyn}}(u; c) = cu^2 + \sqrt{\frac{2}{\pi}} u \exp\left(-\frac{u^2}{2}\right) + 2(1 - u^2)H(u) \quad (33)$$

$$H(u) = \frac{1}{\sqrt{2\pi}} \int_u^\infty dx \exp\left(-\frac{x^2}{2}\right). \quad (34)$$

To simplify notation we denote both  $u_J$  and  $u_K$  as  $u$  in the sequel since there should be no confusion possible.

Stationarity with respect to  $u$  leads to  $c = \text{erfc}(u/\sqrt{2})$ . We remark that when we take the dilution averages to be equal, i.e.,  $c_J = c_K \equiv c$  the dependence on the dilution in (32) factorizes and we simply get an expression equivalent to (30)

$$\frac{\alpha_{\text{asyn}}^{RS}(a, \kappa, c)}{\alpha_{\text{asyn}}^{RS}(a, \kappa, c=1)} = A_{\text{asyn}}(u; c) \quad (35)$$

for any value of the pattern activity  $a$  and stability constant  $\kappa$ .

In order to understand the role of the different couplings in the learning process, we cut them independently and study the influence with varying activity. The results are presented in Fig. 2. We plot the optimal capacity normalized by its value for no dilution,  $\alpha(a, \kappa, c)/\alpha(a, \kappa, 1)$  as a function of the dilution of the  $J$ -couplings,  $c_J$ , for  $c_K = 1$ ,  $\kappa = 0$  and several values of the activity  $a$  (top) and, analogously (bottom) as a function of the dilution of the  $K$ -couplings. We find that when diluting the  $J$ -couplings, referring to the ternary patterns, and keeping all the  $K$ -couplings, related to the active patterns, the normalized capacity decreases as a function of the activ-

ity obtaining the Gardner result for  $a = 1$ . When doing the reverse, the normalized capacity increases as a function of the activity. Moreover, the network is more robust against  $K$ -dilution, especially for large activities. This seems to be quite natural since large activities means many active states  $\pm 1$  such that cutting active patterns becomes relatively less important.

#### IV. DISTRIBUTION OF COUPLINGS

We study the distribution of couplings  $\rho(J, K)$  inside  $V$  in analogy with [15]. This probability distribution can be splitted into two parts, the first one involving the  $(1-c)N$  inactive couplings and the second one,  $\rho_r(J, K)$ , representing the remaining  $cN$  active couplings. Obviously, the first set of couplings is delta distributed so that we can write

$$\rho(J, K) = (1-c)\delta(J)\delta(K) + \rho_r(J, K) \quad (36)$$

where the second set of couplings satisfies

$$\begin{aligned} \rho_r(J, K) = \lim_{N \rightarrow \infty} \left\langle \left\langle \frac{1}{V} \prod_{j=1}^N \text{tr}_{c_j, J_j, K_j} \delta\left(\sum_{i=1}^N c_i J_i^2 - cN\right) \delta\left(\sum_{i=1}^N c_i K_i^2 - cN\right) \times \right. \right. \\ \left. \left. \delta\left(\sum_{i=1}^N c_i - cN\right) \prod_{\mu=1}^p \chi_{\xi_0^\mu}(h^\mu, \theta^\mu; \kappa) \delta(J_1 - J) \delta(K_1 - K) \delta_{c_1, 1} \right\rangle \right\rangle. \end{aligned} \quad (37)$$

In order to compute  $\rho_r(J, K)$  we follow [15] by introducing replicas allowing us to lift the volume  $V$  to the numerator. The calculations are standard but tedious.

Evaluating the expression within the RS approximation we get for synchronous dilution

$$\rho_{r, \text{syn}}(J, K) = \frac{\gamma A_{\text{syn}}(u, \gamma; c)}{2\pi c(1+\gamma)} \exp \left[ -\frac{\gamma A_{\text{syn}}(u, \gamma; c)}{2c(1+\gamma)} (J^2 + K^2) \right] \Theta \left( \frac{\gamma A_{\text{syn}}(u, \gamma; c)}{c(1+\gamma)} \left( J^2 + \frac{K^2}{\gamma} \right) - u^2 \right). \quad (38)$$

This distribution is a two-dimensional Gaussian from which the middle section has been cut out, as represented by the Heaviside function. This gap has an ellipsoidal shape because of the scaling factor  $1/\gamma$  accompanying

the  $K^2$  in the argument. It increases with increasing dilution to reach its maximum when  $c$  tends to zero. In the limit  $\gamma \rightarrow \infty$  this distribution reduces to

$$\lim_{\gamma \rightarrow \infty} \rho_{r, \text{syn}}(J, K) = \frac{A_{\text{syn}}(u, \infty; c)}{2\pi c} \exp \left[ -\frac{A_{\text{syn}}(u, \infty; c)}{2c} (J^2 + K^2) \right] \Theta \left( \frac{A_{\text{syn}}(u, \infty; c)}{c} J^2 - u^2 \right). \quad (39)$$

We remark that this distribution is different from the one obtained in the Gardner case (i.e., the  $a \rightarrow 1$  limit)

because, although the  $K$  couplings do not play any role

for  $\gamma \rightarrow \infty$  the spherical constraint is still present, no matter what the value of  $a$  is.

It is interesting to determine how this probability distribution behaves in the case of no dilution. Then, the distribution (38) for the couplings becomes Gaussian without a gap, viz.

$$\rho_{r,\text{syn}}(J, K; c = 1) = \frac{1}{2\pi} \exp\left(-\frac{J^2}{2} - \frac{K^2}{2}\right). \quad (40)$$

This result is intuitively meaningful since the couplings are forced to obey only the spherical constraint without any restriction coming from the dilution variable. Therefore, we find back the probability distribution for the couplings of the fully connected BEG-perceptron.

For asynchronous dilution a similar treatment can be pursued and we find that the probability distribution for the couplings factorizes

$$\rho_{r,\text{asyn}}(J) = \frac{1}{\sqrt{2\pi}} \sqrt{\frac{A_{\text{asyn}}(c_J, u_J)}{c_J}} \exp\left(-\frac{A_{\text{asyn}}(c_J, u_J)}{2c_J} J^2\right) \Theta\left(|J| - u_J \sqrt{\frac{c_J}{A_{\text{asyn}}(c_J, u_J)}}\right) \quad (41)$$

$$\rho_{r,\text{asyn}}(K) = \frac{1}{\sqrt{2\pi}} \sqrt{\frac{A_{\text{asyn}}(c_K, u_K)}{c_K}} \exp\left(-\frac{A_{\text{asyn}}(c_K, u_K)}{2c_K} K^2\right) \Theta\left(|K| - u_K \sqrt{\frac{c_K}{A_{\text{asyn}}(c_K, u_K)}}\right). \quad (42)$$

These distributions are of a similar nature as the one for the standard diluted perceptron case [15].

## V. DE ALMEIDA-THOULESS STABILITY

Finally, we are interested in studying the local stability of the obtained solutions against RS fluctuations following [6, 17, 21]. From the work on the non-diluted BEG-perceptron [6] we recall that in that case the solutions are unstable only for small activities and very small embedding constants  $\kappa$ . Furthermore, we know that, in general, there are four transverse eigenvalues. In the case of asynchronous dilution these eigenvalues are given by the roots of the fourth degree characteristic polynomial

$$P(\lambda) = \begin{vmatrix} \Delta_q - \lambda & \Delta_c & c_J & 0 \\ \Delta_c & \Delta_r - \lambda & 0 & c_K \\ c_J & 0 & \Delta_{\hat{q}} - \lambda & 0 \\ 0 & c_K & 0 & \Delta_{\hat{r}} - \lambda \end{vmatrix} = 0 \quad (43)$$

where  $\Delta_{\hat{q}}$  and  $\Delta_{\hat{r}}$  read

$$\Delta_{\hat{q}} = \int D(x) \left[ \frac{1}{\hat{q}} \frac{\partial^2}{\partial x^2} \log[1]_{\dagger}(x, E, \hat{q}, \psi_J) \right]^2 \quad (44)$$

$$\Delta_{\hat{r}} = \int D(x) \left[ \frac{1}{\hat{r}} \frac{\partial^2}{\partial x^2} \log[1]_{\dagger}(x, F, \hat{r}, \psi_K) \right]^2 \quad (45)$$

with  $E, F, \phi_J$  and  $\psi_K$  the conjugate variables appearing in the integral representations of the constraints,  $\hat{q}$  and  $\hat{r}$  the conjugate variables of the order parameters  $q$  and  $r$ , and with the short-hand notation

$$[1]_{\dagger}(x, a, b, d) = 1 + \sqrt{\frac{2\pi}{a-b}} \exp\left[-\frac{bx^2}{2(a-b)} - \frac{d}{2}\right].$$

Similar expressions can be written down for  $\Delta_q, \Delta_r$  and  $\Delta_c$  but they are not needed for the argumentation. In-

deed, it is straightforward to check that as soon as dilution is allowed the solution becomes unstable in the saturation limit  $q \rightarrow 1$ . The first derivative of  $[1]_{\dagger}(x, a, b, d)$  has a jump at  $x = u$  proportional to  $u$ , leading to a dirac delta contribution in the second derivative. The square in (44) and (45) forces the replicon eigenvalue to go to  $+\infty$ , similarly to what happens for the standard perceptron model as explained in [22]. When  $u = 0$ , i.e. in the absence of dilution, there is no such delta contribution and we find back the results of [6]. The same reasoning holds for synchronous dilution.

## VI. CONCLUSIONS

In this work we have studied annealed dilution in the BEG perceptron model. Two types of dilution have been discussed, the first one being synchronous dilution, i.e., simultaneous dilution of some of the couplings referring to the ternary patterns themselves and some of the couplings related to the active patterns, the second one being dilution of both these types of couplings independently, so-called asynchronous dilution. We have obtained an analytic formula for the replica symmetric Gardner optimal capacity. For synchronous dilution we see that different regions of activities lead to different results. For small activities  $a \leq 0.5$  the optimal capacity strongly increases for decreasing dilution but normalizing these results by its value for no dilution, the lines for different activities collapse. For large activities  $a \geq 0.6$  the optimal storage capacity is only weakly dependent on the activity but the results for the normalized optimal capacity do not collapse. Furthermore, we see that the network is robust against synchronous dilution for non-sparse coding, i.e., for activities ranging in the interval  $[0.2, 1.0]$ . For asynchronous dilution we find that diluting only the  $J$ -couplings, the normalized optimal capacity decreases as

a function of the activity obtaining the Gardner result for  $a = 1$ . When diluting the  $K$ -couplings, the normalized optimal capacity increases as a function of the activity. Moreover, the network is more robust against  $K$ -dilution, especially for large activities. Since the effects of dilution are of the same order as those in the  $Q = 3$ -Ising model, these results also confirm the better retrieval properties found before for the BEG model.

We have studied the stability of the RS solution against RS breaking fluctuations by generalizing the de Almeida-Thouless analysis. We find that as soon as there is dilution the results are unstable.

### Acknowledgments

We are indebted to Jort van Mourik and Nikos Skantzios for critical and informative discussions. This work has been supported by the Fund of Scientific Research, Flanders-Belgium.

### APPENDIX A

In this appendix we outline the main steps in the calculation of the entropy per neuron (18)-(19).

After defining the order parameters

$$L^\alpha = \frac{1}{\sqrt{cN}} \sum_{j=1}^N c_j^\alpha K_j^\alpha, \quad \forall \alpha \quad (46)$$

$$q_{\alpha\beta} = \frac{1}{cN} \sum_{j=1}^N c_j^\alpha J_j^\alpha c_j^\beta J_j^\beta, \quad \alpha < \beta \quad (47)$$

$$r_{\alpha\beta} = \frac{1}{cN} \sum_{j=1}^N c_j^\alpha K_j^\alpha c_j^\beta K_j^\beta, \quad \alpha < \beta \quad (48)$$

introducing the conjugate order parameters  $\hat{L}^\alpha, \hat{q}_{\alpha\beta}, \hat{r}_{\alpha\beta}$ , and enforcing the constraints (13) and (16) using the Lagrange multipliers  $E^\alpha, F^\alpha$  and  $\hat{\psi}^\alpha$ , we write  $\langle\langle V^n \rangle\rangle$  as the following integral

$$\langle\langle V^n \rangle\rangle = \int \left[ \prod_{\alpha < \beta} \frac{dq_{\alpha\beta} d\hat{q}_{\alpha\beta}}{2\pi i / cN} \frac{dr_{\alpha\beta} d\hat{r}_{\alpha\beta}}{2\pi i / cN} \right] \left[ \prod_{\alpha=1}^n \frac{dL^\alpha d\hat{L}^\alpha}{2\pi / \sqrt{cN}} \frac{dE^\alpha}{4\pi i} \frac{dF^\alpha}{4\pi i} \frac{d\hat{\psi}^\alpha}{4\pi i} \right] \exp[N(G_1 + G_2 + G_3)] \quad (49)$$

where we have defined the functions

$$G_1 = \alpha \log \int \left[ \prod_{\alpha=1}^n \frac{dh^\alpha d\hat{h}^\alpha}{2\pi} \right] \left[ \prod_{\alpha=1}^n \frac{d\theta^\alpha d\hat{\theta}^\alpha}{2\pi} \right] \exp \left[ [i \sum_{\alpha=1}^n (h^\alpha \hat{h}^\alpha + \theta^\alpha \hat{\theta}^\alpha) - ia \sum_{\alpha=1}^n \hat{\theta}^\alpha L^\alpha - \frac{a}{2} \sum_{\alpha, \beta=1}^n \hat{h}^\alpha \hat{h}^\beta q_{\alpha\beta} - \frac{a(1-a)}{2} \sum_{\alpha, \beta=1}^n \hat{\theta}^\alpha \hat{\theta}^\beta r_{\alpha\beta}] \right] \langle\langle \prod_{\alpha=1}^n \chi_{\xi_0}(h_\alpha, \theta_\alpha; \kappa) \rangle\rangle_{\xi_0} \quad (50)$$

$$G_2 = \log \prod_{\alpha=1}^n \text{tr}_{\{c^\alpha, J^\alpha, K^\alpha\}} \exp \left[ - \sum_{\alpha < \beta} \hat{q}_{\alpha\beta} c^\alpha J^\alpha c^\beta J^\beta - \sum_{\alpha < \beta} \hat{r}_{\alpha\beta} c^\alpha K^\alpha c^\beta K^\beta - \frac{1}{2} \sum_{\alpha=1}^n E^\alpha c^\alpha (J^\alpha)^2 - \frac{1}{2} \sum_{\alpha=1}^n F^\alpha c^\alpha (K^\alpha)^2 - \frac{1}{2} \sum_{\alpha=1}^n \hat{\psi}^\alpha c^\alpha \right] \quad (51)$$

$$G_3 = c \sum_{\alpha < \beta} \hat{q}_{\alpha\beta} q_{\alpha\beta} + c \sum_{\alpha < \beta} \hat{r}_{\alpha\beta} r_{\alpha\beta} + \frac{c}{2} \sum_{\alpha=1}^n [E^\alpha + F^\alpha + \hat{\psi}^\alpha]. \quad (52)$$

We have already used that  $\hat{L}^\alpha = 0, \forall \alpha$  at the saddle-point. In the thermodynamic limit  $N \rightarrow \infty$  the entropy is evaluated at the saddle-point for the order parameters (48), the conjugate ones and the Lagrange multipliers  $E^\alpha, F^\alpha$  and  $\hat{\psi}^\alpha$ . Using the RS ansatz for the order pa-

rameters

$$L^\alpha = L \quad E^\alpha = E \quad F^\alpha = F \quad \hat{\psi}^\alpha = \hat{\psi} \quad (53)$$

$$q_{\alpha\beta} = q \quad r_{\alpha\beta} = r \quad \hat{q}_{\alpha\beta} = \hat{q} \quad \hat{r}_{\alpha\beta} = \hat{r} \quad (54)$$

the functions  $G_1, G_2, G_3$  can be simplified further and



the entropy can be written as

---


$$v = -\frac{c}{2}\hat{q}q - \frac{c}{2}\hat{r}r + \frac{c}{2}[E + F + \hat{\psi}] + \int_{-\infty}^{\infty} \mathcal{D}(x, y) \log[1]_{\dagger}(x, y) + \alpha \int_{-\infty}^{\infty} \mathcal{D}(h_0, \theta_0 - l) \langle\langle \log[1]_{\star}^{\xi}(h_0, \theta_0) \rangle\rangle \quad (55)$$

with the short-hand notations

$$[1]_{\dagger}(x, y) = 1 + \frac{2\pi}{\sqrt{(E - \hat{q})(F - \hat{r})}} \exp \left[ -\frac{x^2 \hat{q}}{2(E - \hat{q})} - \frac{y^2 \hat{r}}{2(F - \hat{r})} - \frac{\psi}{2} \right] \quad (56)$$

$$[1]_{\star}^{\xi}(h_0, \theta_0) = \int_{\Omega_{\xi}} \frac{dh}{\sqrt{2\pi(1-q)}} \frac{d\theta}{\sqrt{2\pi(1-r)}} \exp \left[ -\frac{(h - h_0)^2}{2(1-q)} - \frac{(\theta - \theta_0)^2}{2(1-r)} \right] \quad (57)$$


---

where the integral in (57) is restricted to the region  $\Omega_{\xi}$  given by the characteristic function  $\chi_{\xi}(h\sqrt{a}, \theta\sqrt{a(1-a)}; \kappa)$  defined in (15). The RS Gardner optimal capacity is then reached when  $q, r$  go to 1.

At this point we have two choices to proceed. Either we solve numerically the saddle-point equations or we do an asymptotic expansion in the limit  $q, r \rightarrow 1$  in the entropy (55) (or equivalently in the saddle-point equations for the parameters). The first approach has the advantage that we can study  $\alpha$  as a function of  $(q, r)$ . But, since we are only interested in the optimal capacity, we opt for the asymptotic expansion. Since the limits  $q \rightarrow 1$  and  $r \rightarrow 1$  must be taken simultaneously, we introduce a

factor  $\gamma$  such that  $(1 - r) = \gamma(1 - q)$ . Then, a simple inspection of the function (57) appearing in the expression of the entropy (55) suggests that in the limit  $q \rightarrow 1$  this function will diverge as  $(1 - q)^{-1}$ . Since this function is coupled to the capacity and we expect non-trivial results, the other terms in the entropy also have to diverge in such a way. This implies, for instance, that for the function  $[1]_{\dagger}(x, y)$  the terms  $\hat{q}/(E - \hat{q})$ ,  $\hat{\psi}$  and  $\hat{r}/(F - \hat{r})$  appearing in its argument have to go to infinity as  $(1 - q)^{-1}$ . The precise coefficients in front of this divergence are given by the saddle-point equations of the conjugated order-parameters. Performing this asymptotic expansion explicitly leads to the result (20) in Section III.

- 
- [1] M. Blume, V.J. Emery, and R.B. Griffiths, Phys. Rev. A **4**, 1071 (1971); M. Blume, Phys. Rev. **141**, 517 (1966); H.W. Capel, Physica (Amsterdam) **32**, 966 (1966).
  - [2] D.R. Dominguez Carreta and E. Korutcheva, Phys. Rev. E **62**, 2620 (2000).
  - [3] D. Bollé and T. Verbeiren, J. Phys. A: Math. Gen **36**, 295, 2003.
  - [4] D. Bollé, H. Rieger, and G.M. Shim, J. Phys. A: Math. Gen **27**, 3411, 1994.
  - [5] E. Gardner, J. Phys. A: Math. Gen. **21**, 257 (1988).
  - [6] D. Bollé, I. Pérez Castillo, and G. M. Shim, Phys. Rev. E **67**, 036113, 2003.
  - [7] S. Mertens, H. M. Köhler, and S. Bös, J. Phys. A **24**, 4941 (1991).
  - [8] D. Bollé, P. Dupont, and J. van Mourik, Europhys. Lett. **15**, 893 (1991).
  - [9] F. Gerl and U. Krey, J. Phys. A **27**, 7353 (1994).
  - [10] F. Gerl, K. Bauer, and U. Krey, Z. Phys. B **88**, 339 (1992).
  - [11] B. Derrida, E. Gardner, and A. Zippelius, Europhys. Lett **4**, 167 (1987).
  - [12] E. Gardner, J. Phys. A: Math. Gen. **22**, 1969 (1989).
  - [13] B. Wemmenhove and A. C. C. Coolen J. Phys. A: Math. Gen. **63**, 9617 (2003).
  - [14] I. Pérez Castillo and N. Skantzios, cond-mat/0309655
  - [15] M. Bouten, A. Engel, A. Komoda, and R. Serneels, J. Phys. A: Math. Gen **23**, 4643 (1990).
  - [16] D. Bollé and J. van Mourik, J. Phys. A: Math. Gen., **27**, 1151 (1997).
  - [17] M. Mézard, G. Parisi, and M.A. Virasoro, *Spin Glass Theory and Beyond*, Singapore, World Scientific (1987).
  - [18] M.V. Tsodyks, Europhys. Lett. **7**, 203 (1988).
  - [19] C.J. Perez-Vicente, Europhys. Lett. **10**, 621 (1989).
  - [20] H. Horner, Z. Phys. B **75**, 133 (1989).
  - [21] J. R. de Almeida and D. Thouless, J. Phys. A: Math. Gen., **11**, 983 (1978).
  - [22] M. Bouten, J. Phys. A: Math. Gen., **27**, 6021 (1994).